NASA Contractor Report 182082
ICASE Report No. 90–54

ICASE

MULTIGRID FOR HYPERSONIC INVISCID FLOWS

Naomi H. Decker
Eli Turkel

Contract No. NAS1–18605
August 1990

Institute for Computer Applications in Science and Engineering
NASA Langley Research Center
Hampton, Virginia 23665–5225

Operated by the Universities Space Research Association

National Aeronautics and
Space Administration

Langley Research Center
Hampton, Virginia 23665-5225

Multigrid for Hypersonic Inviscid Flows

Naomi Decker †
Eli Turkel ‡ *

† ICASE
NASA Langley Research Center
Hampton Va. 23665
‡ School of Mathematical Sciences
Sackler Faculty of Exact Sciences
Tel-Aviv University
Tel-Aviv 69978, Israel

Abstract

We consider the use of multigrid methods to solve the Euler equations for hypersonic flow. We consider the steady state equations with a Runge-Kutta smoother based on the time accurate equations together with local time stepping and residual smoothing. We examine the effect of the Runge-Kutta coefficients on the convergence rate considering both damping characteristics and convection properties. We also show the importance of boundary conditions on the convergence rate for hypersonic flow. Also of importance are the switch between the second and fourth difference viscosity. Solutions are given for flow around a bump in a channel and flow around a biconic section.

*This research was partially supported by the National Aeronautics and Space Administration under NASA Contract No. NAS1-18605 while the authors were in residence at ICASE, NASA Langley Research Center, Hampton, Va.

Introduction.

Central difference type explicit schemes are currently being applied on a regular basis in the solution of the Euler and Navier-Stokes equations see, e.g [17]. In these applications multigrid is used to accelerate the basic explicit schemes. However, in most cases the applications have been to flows in the transonic or low supersonic regime. Higher speeds have generally been treated without multigrid or using semi-coarsening [8, 10].

Multigrid methods were first developed for elliptic equations. These were later extended to hyperbolic equations such as the fluid dynamic equations for subsonic and transonic flow [4, 7, 12]. For these cases the steady state retains many of the properties of an elliptic equation since the region of supersonic flow is limited. We shall show that with proper care the multigrid method still works for hypersonic flow. Gustafsson and Lotstedt [2] have pointed out that hyperbolic multigrid works by two different processes. For the long waves the advection process is most important and multigrid achieves its efficiency by allowing the use of larger time steps on coarser grids. Hence, it is important that the smoother use large time steps. However, for the shorter waves dissipation is more important and the efficiency of multigrid is based on principles similar to that for elliptic equations. In this study we consider a Runge-Kutta scheme [3] as the smoother for the multigrid method. The central differences are augmented by an artificial viscosity based on TVD principles [13]. A number of changes are made to the scheme to enable it to work for higher speed flows. We consider both unbounded domains and domains with solid surfaces at the boundaries. The main difficulties are not due to the basic multigrid method but rather to the imposition of boundary conditions. We first describe the basic Runge-Kutta method for the central difference scheme together with a description of the artificial viscosity. We then describe the theory of the multigrid acceleration for a simple advection equation. We finally present several examples to demonstrate our conclusions.

Basic Scheme

The basic elements of the scalar dissipation model considered in this paper were first introduced by Jameson, Schmidt, and Turkel [3] in conjunction with Runge-Kutta explicit schemes. The space discretization is based on central differences with an additional artificial viscosity. This algorithm has been used by many investigators to numerically solve the Euler equations for a wide range of fluid dynamic applications. The same type of space discretization has been applied to alternating direction implicit (ADI) schemes [9] and LU factored implicit schemes [5]. In this section the basic scheme is briefly reviewed.

Consider the Euler equations in the form

$$W_t + f_x + g_y = 0, \tag{1}$$

where W is the four-component vector of conserved variables, and f, g are the flux vectors. The independent variables are time t and Cartesian coordinates (x, y). If (1) is transformed to arbitrary curvilinear coordinates $\xi = \xi(x, y)$ and $\eta = \eta(x, y)$, then we obtain

$$(J^{-1}W)_t + F_\xi + G_\eta = 0 \tag{2}$$

where J^{-1} is the inverse transformation Jacobian, and

$$F = fy_\eta - gx_\eta, \qquad G = gx_\xi - fy_\xi.$$

In a cell-centered, finite-volume method, (1) is integrated over an elemental volume in the discretized computational domain, and J^{-1} is identified as the volume of the cell. Equation (2) can also be written as

$$J^{-1}W_t + AW_\xi + BW_\eta = 0$$

where A and B are the flux Jacobian matrices defined by $A = \partial F/\partial W$ and $B = \partial G/\partial W$.

To advance the scheme in time we use a multistage scheme. A typical step of a Runge-Kutta approximation to (2.2) is

$$W^{(k)} = W^{(0)} - \alpha_k \frac{\Delta t}{J^{-1}} \left[D_\xi F^{(k-1)} + D_\eta G^{(k-1)} - AD \right], \tag{3}$$

where D_ξ and D_η are spatial differencing operators, and AD represents the artificial dissipation terms. The derivatives of the fluxes are approximated by central differences. Hence, we need to evaluate F at $(i+\frac{1}{2})$. Since the dependent variables are given at (i,j) we need to average them to calculate the flux at the cell face. This averaging can be done in several ways. In the original code the conservative variables were averaged to find the variables at the cell face and then the flux was evaluated. Some care must be taken with the geometric terms so that a constant field yields a zero derivative. In fact for the two dimensional case 5 quantities were averaged, the four conservative variables and $E + p$. This was done because of enthalpy damping. Alternatively one can average density, momentum and total enthalpy. This might be more accurate since the total enthalpy is constant in the steady state. An alternative to this procedure is to average the fluxes rather than the dependent variables again with modifications for metric terms. Averaging the fluxes allows for a more accurate representation of the Rankine-Hugoniot jump condition in one dimension. In this study we average the fluxes but have not seen much difference between the various approaches.

The dissipation terms are a blending of second and fourth differences. That is,

$$AD = \left(D_\xi^2 + D_\eta^2 - D_\xi^4 - D_\eta^4 \right) W, \tag{4}$$

where

$$D_\xi^2 W = \nabla_\xi \left[\left(\lambda_{\xi_{i+\frac{1}{2},j}} \epsilon^{(2)}_{i+\frac{1}{2},j} \right) \Delta_\xi \right] W_{i,j}, \tag{5}$$

$$D_\xi^4 W = \nabla_\xi \left[\left(\lambda_{\xi_{i+\frac{1}{2},j}} \epsilon^{(4)}_{i+\frac{1}{2},j} \right) \Delta_\xi \nabla_\xi \Delta_\xi \right] W_{i,j}, \tag{6}$$

and Δ_ξ , ∇_ξ are the standard forward and backward difference operators respectively associated with the ξ direction. The variable scaling factor λ is chosen as

$$\lambda_{\xi_{i+\frac{1}{2},j}} = \frac{1}{2} \left[(\lambda_\xi)_{i,j} + (\lambda_\xi)_{i+1,j} \right], \tag{7}$$

where λ_ξ is proportional to the spectral radius of the matrix A. The coefficients $\epsilon^{(2)}$ and $\epsilon^{(4)}$ are adapted to the flow and are defined as follows:

$$\epsilon^{(2)}_{i+\frac{1}{2},j} = \kappa^{(2)} \max(\nu_{i-1,j}, \nu_{i,j}, \nu_{i+1,j}, \nu_{i+2,j}), \tag{8}$$

$$\nu_{i,j} = \left| \frac{p_{i+1,j} - 2p_{i,j} + p_{i-1,j}}{p_{i+1,j} + 2p_{i,j} + p_{i-1,j}} \right|, \tag{9}$$

$$\epsilon^{(4)}_{i+\frac{1}{2},j} = \max\left[0, \left(\kappa^{(4)} - \epsilon^{(2)}_{i+\frac{1}{2},j}\right)\right], \tag{10}$$

where p is the pressure, and the quantities $\kappa^{(2)}$ and $\kappa^{(4)}$ are constants to be specified. The operators for the η direction are defined in a similar manner.

The second-difference dissipation term is nonlinear. Its purpose is to introduce an entropy-like condition and to suppress oscillations in the neighborhood of shocks. This term is small in the smooth portion of the flow field. The fourth-difference dissipation term is basically linear and is included to damp high-frequency modes and allow the scheme to approach a steady state. Only this term affects the linear stability of the scheme. Near shocks it is reduced to zero.

For high speed flows the switch (9) is not very good and does not allow the multigrid to converge. Instead we consider a TVD variation of the switch [13] given by

$$\nu_{i,j} = \frac{|p_{j+1} - 2p_j + p_{j-1}|}{|p_{j+1} - p_j| + |p_j - p_{j-1}| + \epsilon}, \quad \kappa^{(2)} = 1/2. \tag{11}$$

With this change and the factor $1/2$ in front of the second-difference dissipation term, the scalar equation becomes first-order upwind near shocks. In the case of the original ν we find that $\nu \simeq .05$ near shock waves in transonic flows. ϵ must be chosen carefully to prevent the switch from being activated by noise.

We now no longer have a free parameter for the second-difference dissipation. We also replace (10) by

$$\epsilon^{(4)}_{i+\frac{1}{2},j} = \max\left[0, \kappa^{(4)}\left(1 - \Gamma\epsilon^{(2)}_{i+\frac{1}{2},j}\right)\right], \tag{12}$$

We choose $\Gamma = 2$ so that the fourth-difference dissipation is cut off for $\nu \geq 1/2$. The only free parameter is the coefficient $\kappa^{(4)}$ of the fourth-difference term.

Several other changes were made to the code in addition to the change to a TVD switch. In the original algorithm the artificial viscosity for the energy equation was based on the total energy rather than the energy. For high speed flows we base the artificial viscosity on the energy so that in each equation the basic dependent variable is also used in the artificial viscosity. This is more in line with upwind codes. This has previously been used in central difference codes [1]. The algorithm no longer preserves a constant total enthalpy in the steady state but enthalpy damping is not useful for supersonic flows. In most cases the difference between the two approaches is small with each approach having its advantages. The original version seems to give slightly sharper shocks.

To facilitate the treatment of boundaries, two layers of ghosts cells are created near each boundary. These ghosts cells are calculated by some extrapolation technique and then central difference are used at all interior points for the fluxes and artificial viscosities. At the solid boundary the normal velocity is reflected antisymmetrically to all ghost cells while the tangential velocity and density is reflected symmetrically to all ghosts cells. The pressure is calculated by the normal momentum equation. Hence, no special logic is required for the artificial viscosity near the solid surface. This procedure was found to be superior to setting the using zeroth order extrapolation for the first differences and setting the third difference equal to zero in calculating the artificial viscosity at the wall. We have also found that the effect of the second difference (5) is much more important near the solid surface than the fourth difference (6). Hence, there is no harm at setting the third difference equal to zero near the wall.

We finally discuss the choice of the Runge-Kutta parameters α_k and the time step in (3). For the coarser meshes and a scalar equation the central difference scheme with the artificial viscosity reduces to a first order upwind scheme. For this scheme TVD parameters have been suggested by Shu [11]. Tai [15, 18] has suggested other parameters that are optimal for damping characteristics. We have generally followed the suggestions of Tai as detailed later though the differences between the two set of coefficients was small. On the fine mesh we have a difficulty since in the smooth regions the scheme is a central difference operator with a fourth difference viscosity. However, near shocks the switch reduces the scheme to a first order upwind scheme. Hence, we have chosen Runge-Kutta coefficients that are stable for both sets of schemes. For most of the cases described below we have used a three stage Runge-Kutta time stepping scheme. On the coarser meshes we first considered the coefficients $\alpha_1 = 1/9, \alpha_2 = 1/3$ and $\alpha_3 = 1$. This has the property that for CFL $= 3$ we have pure convection, i.e. the wave moves one cell each stage without any dissipation. We then reduce the CFL to 1.5 to introduce dissipation. This turns out to be the same parameters suggested by Shu in his TVD scheme. After some experimentation we now choose $\alpha_1 = .148, \alpha_2 = .4$ and $\alpha_3 = 1$ with no residual smoothing and CFL $= 1.5$ as suggested by Tai. On the finest mesh we choose $\alpha_1 = .2, \alpha_2 = .55$ and $\alpha_3 = 1$ with a constant residual smoothing parameter $\beta = .2$ and $CFL = 2.5$. In all cases the artificial viscosity was updated at every stage.

We have also experimented with a time step that depends on $\nu_{i,j}$ as given in (11). In this case the time step is smaller near strong shocks. We have also increased the second order difference on the coarser meshes by introducing a dependence on ν, see also [10].

Multigrid

Although we are primarily interested in solving the Euler equations, the simple advection equation provides useful clues to the role of multigrid for accelerating the convergence. We next describe the multigrid theory for both the one and two dimensional model problems. The one dimensional analysis is used to motivate the choice of Runge-Kutta parameters and time step. The two dimensional analysis indicates the central role of the boundary conditions.

One dimensional theory

Each Runge Kutta iteration has the potential to both convect and damp the error. In a multigrid scheme, the damping of the higher frequency errors is an essential property of the smoother. Lower frequency errors are more efficiently damped on coarser grids. For a fixed time step the convergence of the multigrid method is improved as the damping properties of the smoother are improved. On the other hand, to get the most advantage from the convective properties of the Runge Kutta scheme, a large time step is needed. An increase in the time step is often at the expense of the efficiency of the smoothing. To quantify these observations, we consider the one dimensional scalar advection problem

$$u_t + u_x = 0. \tag{13}$$

We first analyze the periodic boundary condition case, where the Runge Kutta multigrid scheme is optimized by considering only the damping properties of the RK smoother – convection cannot accelerate convergence. After discretizing the spatial derivative using a central difference on a uniform mesh and adding both first and third order artificial viscosities, see (5) and (6). We rewrite equation (3) as

$$u^{(k)} = u^{(0)} - \alpha_k \Delta t R^{(k-1)} \tag{14}$$

where

$$\begin{aligned}(R^{(k-1)})_i &= \frac{u_{i+1} - u_{i-1}}{2\Delta x} - \epsilon^{(2)}\Delta x \frac{u_{i+1} - 2u_i + u_{i-1}}{(\Delta x)^2} \\ &\quad + \epsilon^{(4)}(\Delta x)^3 \frac{u_{i+2} - 4u_{i-1} + 6u_i - 4u_{i+1} + u_{i-1}}{(\Delta x)^4}.\end{aligned}$$

The convergence properties of the time iteration (used to solve the periodic problem) can be studied by looking at the amplification factor. If $\hat{u} = e^{i\theta x/\Delta x}$ is a Fourier mode, then the symbol of the residual is

$$\hat{R}(\theta) = \frac{1}{\Delta x}[i \sin\theta + 4\epsilon^{(2)} \sin^2\theta + 16\epsilon^{(4)} \sin^4\theta] \tag{15}$$

and the symbol for the complete, k stage Runge-Kutta iteration is

$$\hat{u}^{n+1} = g(\theta)\hat{u}^n \tag{16}$$

where

$$g(\theta) = 1 + \alpha_k z + \alpha_k\alpha_{k-1}z^2 + \cdots + \alpha_k\alpha_{k-1}\cdots\alpha_1 z^k$$

and

$$z = -\Delta t \hat{R}(\theta).$$

For low frequency errors, $|\theta| << 1$, the symbol of the residual is also small. In fact,

$$z \approx -\lambda(i\theta + 4\epsilon^{(2)}\theta^2), \qquad \lambda = \frac{\Delta t}{\Delta x}$$

and therefore $|g(\theta)|$ is close to one. Thus, low frequency errors are reduced very slowly. For high frequency errors, the size of $|g(\theta)|$ depends on the Runge-Kutta parameters as well as on the Courant number. To use the RK time stepping scheme effectively as a multigrid smoother, the amplification factor should be small for all frequencies which cannot be represented on coarser levels, i.e. the high frequencies. Various strategies, based on this model problem, have been used to obtain parameters which result in good Runge-Kutta smoothers. The basic philosophy is to uniformly reduce the amplification factor over all high frequencies, $\pi/2 \leq \theta \leq \pi$. We note, however, that the choices of the alpha's and the Courant number depend very strongly on the type and strength of the dissipation terms. Optimal choices for a three stage scheme for the first order upwind discretization ($\epsilon^{(2)} = 1/2, \epsilon^{(4)} = 0$), for instance, results in an unstable scheme when used for the third order discretization with $\epsilon^{(2)} = 0, \epsilon^{(4)} = 1/16$.

For linear problems, the multigrid algorithm consists of both the RK smoother and a coarse grid correction. In a typical two grid scheme, the coarse grid correction involves the restriction of the residual to a coarse level, solving for the correction on the coarse level, and then interpolation of the correction back to the fine grid. Multiple level schemes replace the coarse grid solve by another RK step together with a coarse grid correction to the next coarser level. Using reasonably good RK parameters with suitable restriction, interpolation and coarse grid operators results in a one dimensional iterative method which converges uniformly well for all mesh sizes. Moreover, the convergence per multigrid cycle can be made arbitrarily good using a RK smoother with a sufficient number of stages. This is not necessarily the case for the two dimensional problem, as we explain below.

Two dimensional theory

We now consider the two dimensional advection problem,

$$u_t + au_x + bu_y = 0, \tag{17}$$

first with periodic boundary conditions. Although the one dimensional analysis of the RK scheme can be used to get stable 2-d RK schemes, the two dimensional coarse grid correction is fundamentally different than in one dimension. There are low frequency errors whose residuals are magnified on coarser grids. The easiest way to understand this is the following. Suppose the space derivatives have been discretized on a uniform grid with cells of size $h \times h$ as in the one dimensional case, a central difference plus artificial viscosity in the form of both second and fourth differences. Then the Fourier symbol, corresponding to a Fourier mode, $e^{i\theta x/h}e^{i\phi y/h}$, of the two dimensional residual is

$$h\hat{R}_h(\theta,\phi) = i(a\sin\theta + b\sin\phi) + 4\epsilon^{(2)}(a\sin^2\theta + b\sin^2\phi) + 16\epsilon^{(4)}(a\sin^4\theta + b\sin^4\phi)$$

which, for small θ and ϕ, is

$$\approx i(a\theta + b\phi) + 4\epsilon^{(2)}(a\theta^2 + b\phi^2) + 16\epsilon^{(4)}(a\theta^4 + b\phi^4). \tag{18}$$

On the coarser grid, with cells of size $2h \times 2h$, the symbol of the residual for the same frequency is

$$h\hat{R}_{2h}(\theta,\phi) = \frac{i(a\sin 2\theta + b\sin 2\phi)}{2} + 4h(2h)\epsilon^{(2)}\frac{(a\sin^2 2\theta + b\sin^2 2\phi)}{(2h)^2} + 16h(2h)^3\epsilon^{(4)}\frac{(a\sin^4 2\theta + b\sin^4 2\phi)}{(2h)^4}.$$

For small θ and ϕ this is approximately

$$\approx i(a\theta + b\phi) + 8\epsilon^{(2)}(a\theta^2 + b\phi^2) + 128\epsilon^{(4)}(a\theta^4 + b\phi^4). \tag{19}$$

Several observations can be made by comparing these two symbols, one representing the residual on the fine grid and the other representing the residual of the same error on a coarse grid. The Runge Kutta smoother cannot efficiently damp the low frequency errors. At the same time, the restriction and the interpolation operators transfer the low frequencies quite accurately. Thus, a two level multigrid cycle, even assuming that the coarse grid equations are solved exactly, can only solve for the lowest frequencies to the extent to which they can be represented on the coarse grid. Comparing the two expressions (18) and (19), we see the following. If $a\theta + b\phi \geq Ch$ for some positive constant, C, then the first term in both expressions is the dominant term, and the expressions are approximately equal. Thus the coarse grid 'sees' the same residual, and can correct for it. However, if $a\theta + b\phi$ is zero, i.e., the error is constant along characteristics, the imaginary part of the symbol vanishes and the situation is quite different. If only first order viscosity (i.e., $\epsilon^{(2)} \neq 0$, $\epsilon^{(4)} = 0$) is used on both the fine and the coarse grids, then, for small θ and ϕ, the ratio of the size of the residual when computed on the fine grid to the size of the residual computed on the coarse grid is

$$\approx \frac{4\epsilon^{(2)}(a\theta^2 + b\phi^2)}{8\epsilon^{(2)}(a\theta^2 + b\phi^2)} = \frac{1}{2}.$$

If only the third order viscosity is used on both fine and coarse grids (i.e., $\epsilon^{(2)} = 0$, $\epsilon^{(4)} \neq 0$), then this ratio is only

$$\approx \frac{16\epsilon^{(4)}(a\theta^4 + b\phi^4)}{128\epsilon^{(4)}(a\theta^4 + b\phi^4)} = \frac{1}{8}.$$

Since it is common to use the higher order viscosity on fine grids, and the less expensive, lower order viscosity on coarse grids, we also consider the case where $\epsilon^{(2)} = 0$ and $\epsilon^{(4)} \neq 0$ on the fine grid and $\epsilon^{(2)} \neq 0$ and $\epsilon^{(4)} = 0$ on the coarse grid. In this case, the ratio is

$$\approx \frac{16\epsilon^{(4)}(a\theta^4 + b\phi^4)}{8\epsilon^{(2)}(a\theta^2 + b\phi^2)} << 1$$

Thus the corresponding multigrid algorithms will only be able to reduce the errors which are constant along characteristics by the approximate amounts of 1/2, 7/8 and 1 (not

at all), depending on the type of viscosities used. In particular, we note that this means that, no matter how well the RK scheme is optimized, the convergence rate per multigrid cycle cannot be made arbitrarily small.

For non-periodic boundary conditions, for example those used for inflow/outflow or at a solid body, the situation is not as bad. In this case, convection plays an important role in the convergence process. To see the effect of inflow/outflow boundary conditions on the convergence rates of the multigrid, consider the two dimensional advection equation, (17) on the unit square, with $a = b = 1$ with inflow boundary conditions specified at the bottom and left sides. Table 1 shows the difference in the convergence rates of the periodic problem and the inflow/outflow problem for a two grid multigrid algorithm. The computations were done by explicitly forming all of the matrices involved and then finding the eigenvalue of greatest modulus. We used the same RK coefficients for all cases, with $\alpha_1 = .2$, $\alpha_2 = .55$, $\alpha_3 = 1$ and $\lambda = 1.5$. The coarse grid equations are solved exactly. The spectral radii are given for one to three RK smoothing steps per multigrid cycle. Table 1a is with $\epsilon^{(2)} = 1/2$, $\epsilon^{(4)} = 0$ on the fine grid and $\epsilon^{(2)} = 1/2$, $\epsilon^{(4)} = 0$ on the coarse grid, Table 1b is with $\epsilon^{(2)} = 0$, $\epsilon^{(4)} = 1/16$ on the fine grid and $\epsilon^{(2)} = 0$, $\epsilon^{(4)} = 1/16$ on the coarse grid, and Table 1c is with $\epsilon^{(2)} = 0$, $\epsilon^{(4)} = 1/16$ on the fine grid and $\epsilon^{(2)} = 1/2$, $\epsilon^{(4)} = 0$ on the coarse grid. We make the following observations. The convergence rates of the inflow/outflow problems are much better than for the corresponding periodic problems. Rather surprisingly, the numbers indicate that this is true even as the problem size is increased. This effect is much greater than can be attributed to just the convection on the fine grid, since this would just reduce the convergence rate by a factor of $1 - O(h)$. Moreover, additional smoothing can be used to further reduce the convergence rate for the inflow/outflow problem.

Model problem vs. real problem

To what extent does the model problem analysis predict the behavior for our real problem of interest? In the model problem analysis we have tried to model the multigrid cycle as closely as possible. For the Euler equations, we use a cell-centered FAS multigrid approach for non-linear equations to accelerate the convergence of the Runge-Kutta time stepping to the steady state solution. For linear problems such as our model advection problem, FAS is equivalent to the correction scheme. A cell-centered scheme was used in both cases, with equivalent projection and interpolation operators for the case of uniform grids. There are many differences, however, which are more difficult to model. We mention a few of them here.

Since the choice of the RK parameters depends strongly on the amount of artificial dissipation, it is somewhat surprising that the model problem parameters work at all for the Euler equations. A scalar viscosity is used for the system, the same amount for each equation. Thus the effective sizes of $\epsilon^{(2)}$ and $\epsilon^{(4)}$ which would be appropriate in the model problem analysis actually lie in a range of values. Similarly, although we use local time stepping, the Courant number, λ^* is a scalar quantity determined by the whole system and used for all four equations. Thus, the model problem should also be analyzed for a whole range of λ's. The use of the nonlinear switching mechanism on the fine grid also

a).

RK steps	periodic			inflow/outflow		
	8×8	16×16	32×32	8×8	16×16	32×32
1	.567	.591	.607	.371	.378	.381
2	.517	.519	.513	.138	.145	.154
3	.498	.515	.511	.068	.089	.096

b).

RK steps	periodic			inflow/outflow		
	8×8	16×16	32×32	8×8	16×16	32×32
1	.888	.919	.933	.685	.704	.709
2	.859	.898	.919	.477	.507	.527
3	.838	.890	.900	.333	.364	.399

c).

RK steps	periodic			inflow/outflow		
	8×8	16×16	32×32	8×8	16×16	32×32
1	.951	.990	.998	.697	.748	.768
2	.929	.988	.997	.496	.528	.547
3	.911	.986	.997	.354	.389	.401

Table 1: Comparisons of spectral radii for two grid multigrid, periodic vs. inflow/outflow a). first order discretization on both fine and coarse grid levels b). third order discretization on both fine and coarse grid levels c). third order discretization on fine and first order on coarse grid level

complicates the correspondence between the artificial viscosities for the model and real problems. Thus, for smooth flows, the model problem using $\epsilon^{(2)} = 0$ on the fine grid and $\epsilon^{(4)} = 0$ on the coarse grids has similar behavior. The non-uniform mesh with varying aspect ratios of the cells and the variation in the alignment of the flow with the grid can be partially modeled by considering the 2-d advection equation (17) with varying ratio, a/b.

Results

In all cases we use a 3 stage formula as described above. A simple V cycle is used with smoothing on the way down to coarser meshes and simple interpolation on the way up to finer meshes. The standard formula is to do one smooth on the finest mesh and 2 smoothings are all coarser meshes, though other choices are described later. The coefficient of the third order viscosity is $\kappa^{(4)} = 1/16$.

We first consider an inflow-outflow case. We use a uniform Cartesian grid with a constant inflow at the left and lower boundaries and outflow at the right and top boundaries. The Mach number and angle of attack are used to specify the three incoming

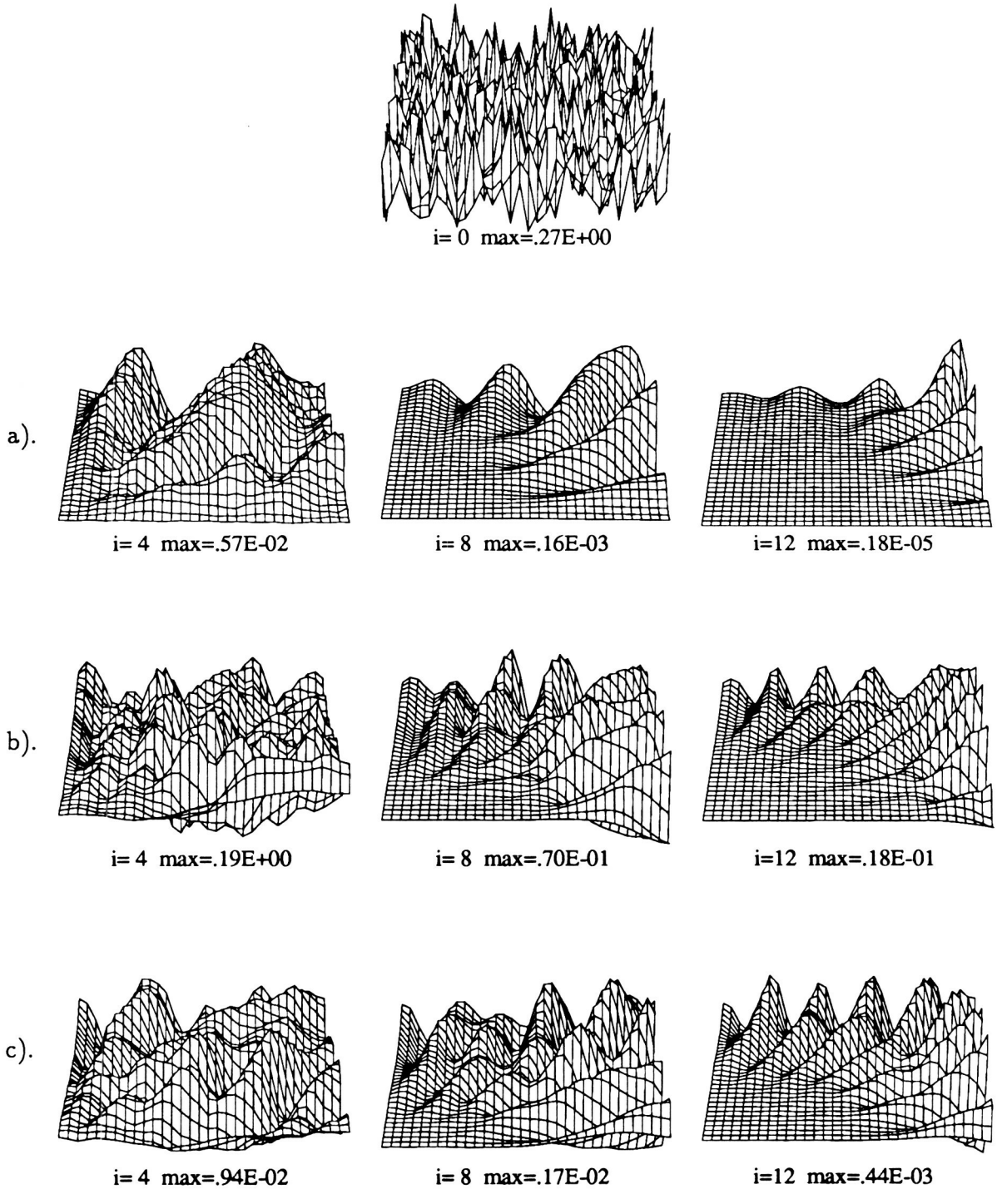

Figure 1: Entropy in inflow/outflow case, Mach 10, 45 degree angle: a) first order viscosity on fine and all coarse levels b) third order viscosity on fine and all coarse levels c) switched viscosity on fine grid and first order viscosity on all coarse levels.

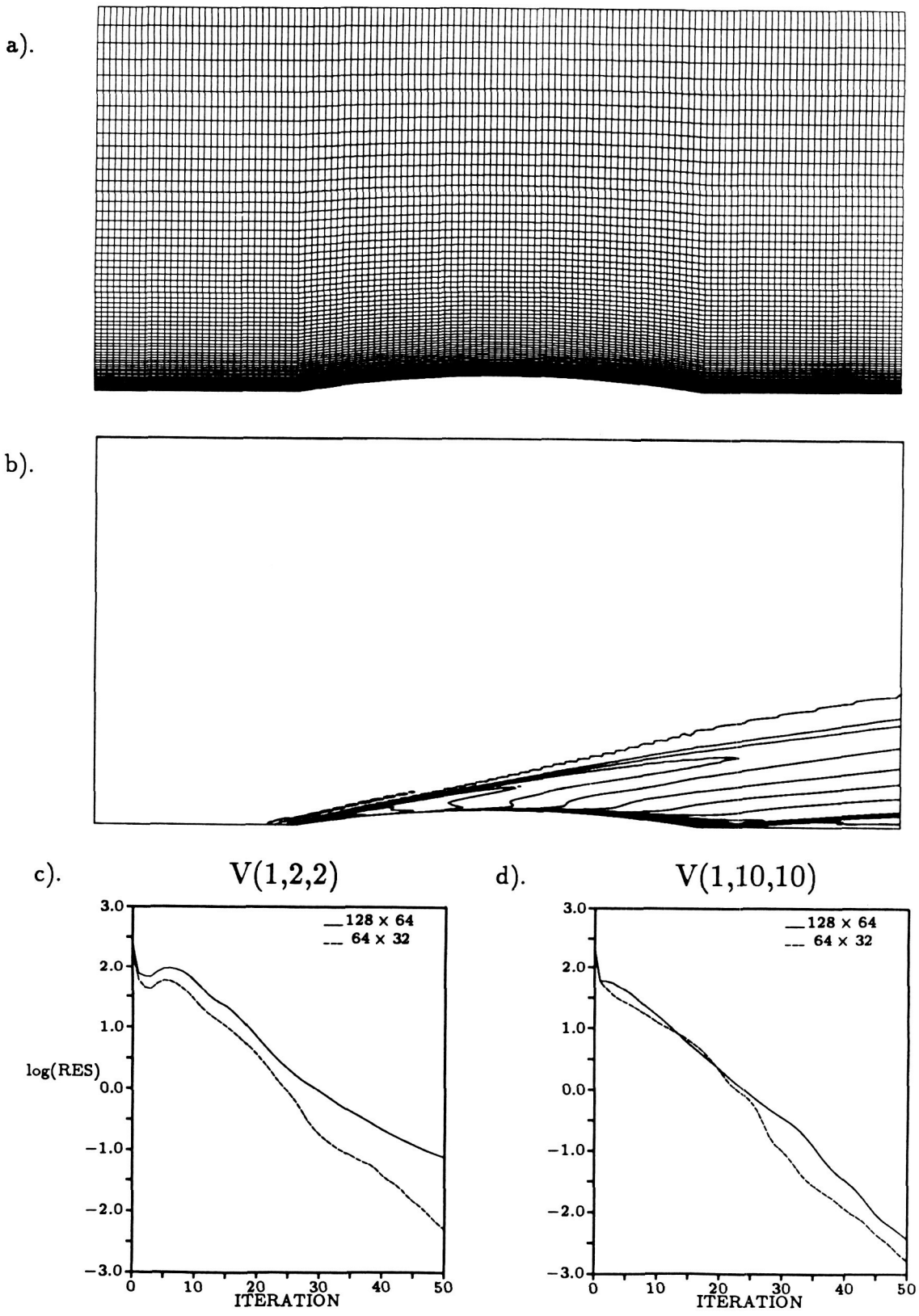

Figure 2: Flow over a bump in a channel, Mach 10

characteristic variables at inflow while the outgoing variable is extrapolated from the interior. At outflow one characteristic is incoming and is specified while the other three are extrapolated. The steady state solution is a constant. The initial conditions are the steady state solution plus a ten percent random perturbation. In figure 1 we plot the entropy for a flow entering the domain at 45 degrees to the x axis and a speed of Mach 10 after 4, 8 and 16 multigrid cycles. One can clearly see that the main wave travels along the characteristics which for the entropy is the stream line, with the convergence rates consistent with the theoretical results for the two dimensional advection equation with various artificial viscosities. The effect of the advection is clearly seen.

In the second case we consider flow in a channel with a 4 percent bump on the lower wall. The grid is uniform in the x direction and stretched in the y direction. In figure 2a we show the grid while in figure 2b we plot the isomach lines for a Mach 10 flow. In figure 2c we show the convergence rate for both a 64×32 grid and a 128×64 grid with the standard multigrid parameters. In figure 2d we plot the convergence rate when we do one iteration on the finest mesh and 10 iterations on the coarser meshes instead of the standard 2 iterations on the coarser mesh. We see that doing more iterations on the coarser meshes does not do any harm. On the contrary in figure 2d we have a convergence rate independent of mesh size which we did not have in figure 2c.

In the third case we consider flow about a cone consisting of two sections. The mesh is 128×32 with a nonuniform grid. The inflow is at Mach 6 with 0 degree angle of attack. In figure 3a we plot the convergence history for this case. In figure 3b we plot the residual of the continuity equation when the standard multigrid parameters are used. We have plotted both the entire field and a closeup of the leading edge. As expected the largest contributions to the residual come from the bow shock and two weaker shocks that originate at the point where the cone has a discontinuous tangent. In figure 3c we perform only one smoothing on the coarser grids. There is now a noticeable residual ahead of the bow shock in the free stream region. Thus, this multigrid scheme has caused disturbances to move upstream while in figure 3b there are only minor perturbations ahead of the shock. Hence, the central difference scheme allows disturbances to propagate upstream but the net effect is negligible. Hence, if the central multigrid acceleration does not contain enough smoothing on all grids then it can increase the effect of this upstream perturbation. Hence, there may be an advantage to considering an upwind multigrid even for central difference schemes.

Conclusions

The efficiency of multigrid for the Euler equations is governed by the smoothing properties of the basic scheme perpendicular to the characteristics and to convection properties of the scheme along the characteristics. On the coarse grids we have used Runge-Kutta parameters that are optimal for first order upwind schemes. On the finest mesh we use parameters that are stable for both a first order upwind scheme and a central difference scheme with a fourth difference artificial viscosity. By using residual smoothing we can increase the time step while maintaining good smoothing properties. In general

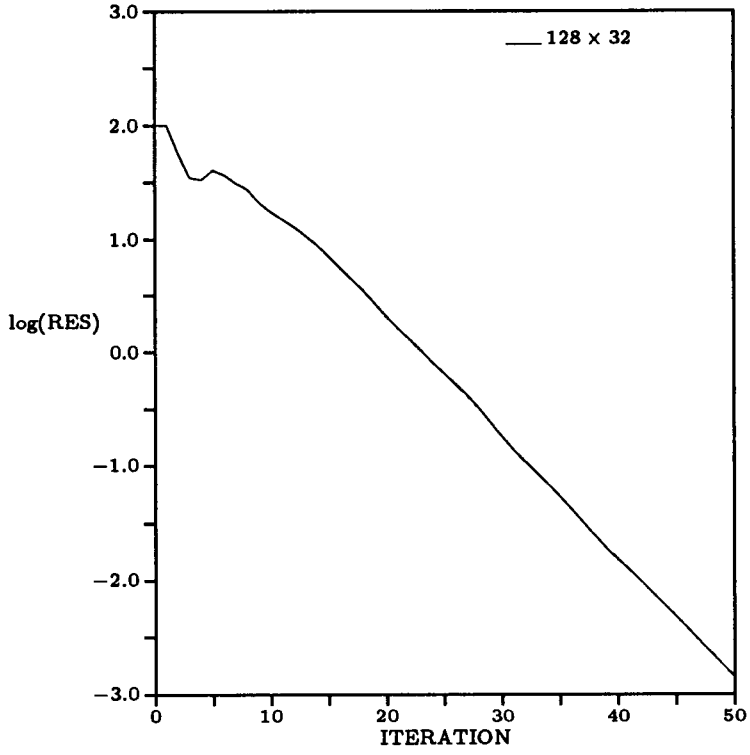

Figure 3a

b).

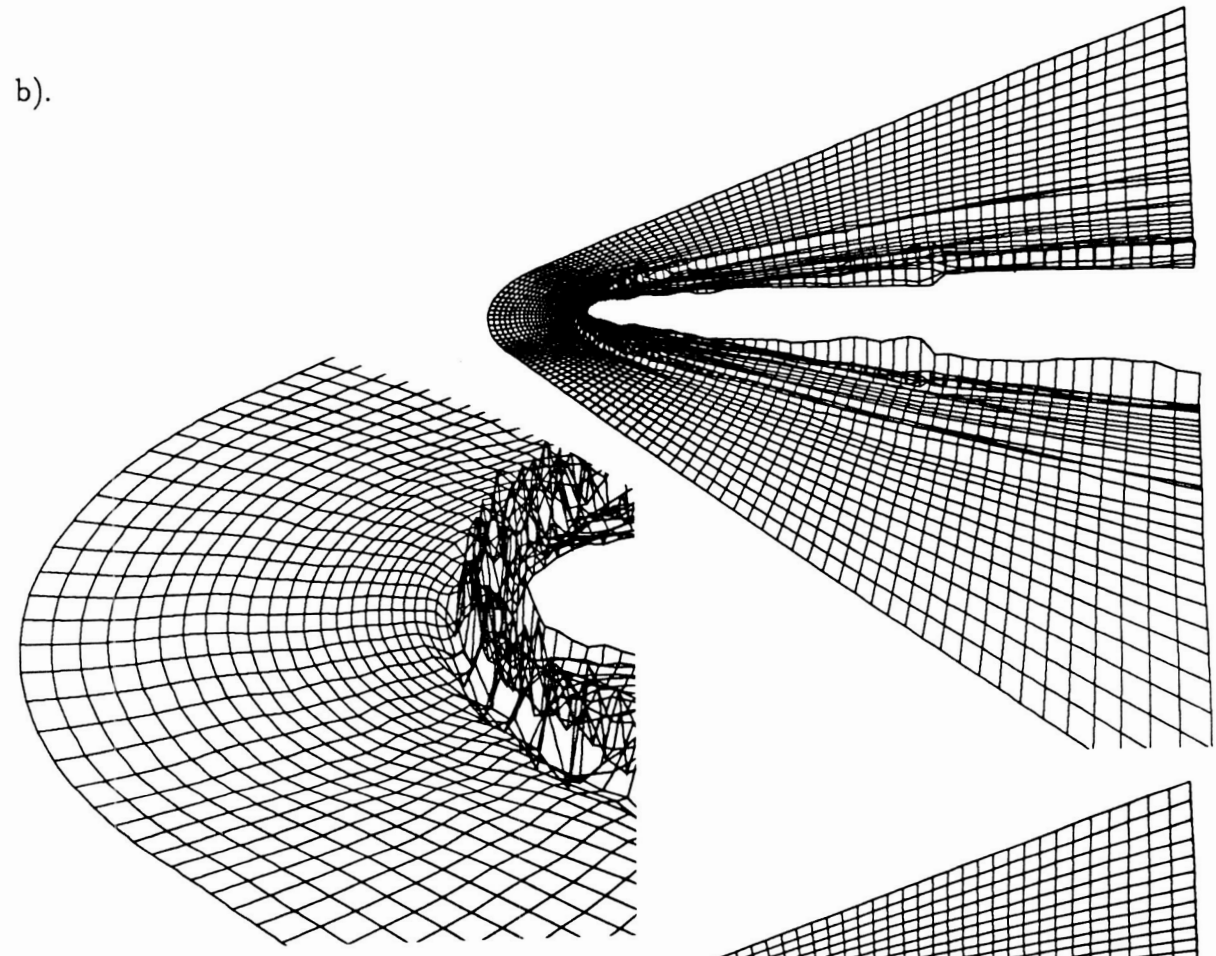

c).

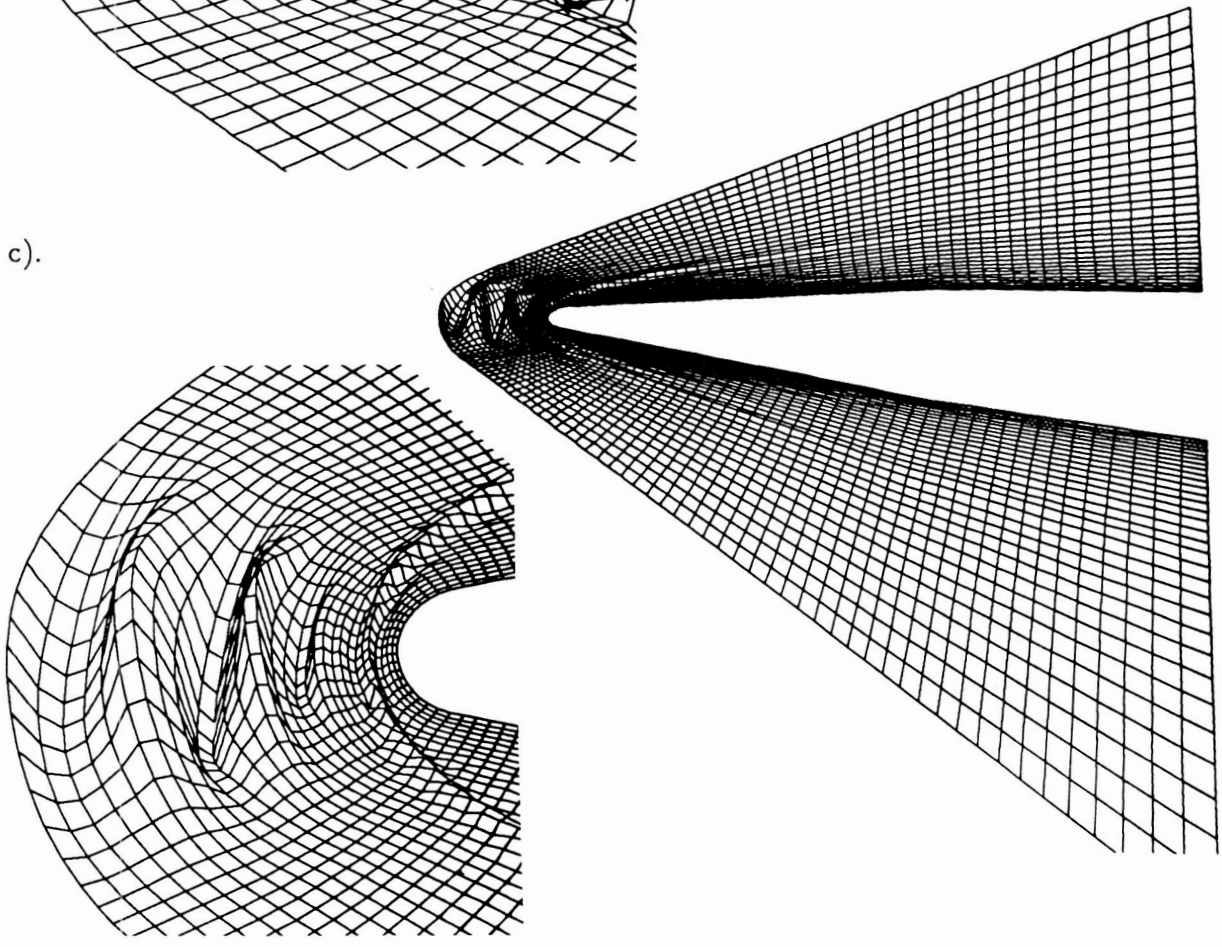

Figure 3: Flow over a cone, Mach 6

we have found that a small amount of residual smoothing increased the robustness of the code. However, further increasing the residual smoothing and increasing the time step did not seem to improve the convergence rate. For a central difference scheme with artificial viscosity the second difference viscosity is important for the shock treatment. The behavior of the multigrid scheme is more affected by the fourth difference viscosity. Hence, a TVD scheme by itself is not a good smoother for a multigrid scheme until extra terms are added that can damp high frequencies.

We have found that for inflow-outflow boundaries that the multigrid central difference scheme converges rapidly for all Mach numbers. We have indeed shown that the convergence rates for the semi-infinite case are better than for the periodic case. The difficulties and slow convergence rates for more difficult geometries are due to boundary treatment. Care must all be exercised in the treatment of the artificial viscosity near the boundary. For the inflow-outflow case computing many iterations of the smoother on the coarse grids increases the convergence rate but not by very much so that it is not efficient. One drawback of the multigrid method is that it can convect disturbances upstream even for hypersonic problems. This propagation against the stream can be more pronounced than that introduced by the central difference smoother.

References

[1] Caughey, D.A. and Turkel, E., *Effects of Numerical Dissipation on Finite-Volume Solutions to Compressible Flow Problems,* AIAA Paper 88-0621, 1988.

[2] Gustafsson, B. and Lotstedt, P., *Analysis of the Multigrid Method Applied to First Order Systems,* Proceedings Fourth Copper Mountain Conference on Multigrid Methods, ed. by J. Mandel et. al., SIAM, Philadelphia, 1990.

[3] Jameson, A., Schmidt, W., and Turkel, E., *Numerical Solutions of the Euler Equations by Finite Volume Methods Using Runge-Kutta Time-Stepping Schemes,* AIAA Paper 81-1259, 1981.

[4] Jameson, A. and Baker, T. J., *Multigrid Solution of the Euler Equations for Aircraft Configurations,* AIAA Paper 84-0093, 1984.

[5] Jameson, A. and Yoon, S., *Lower-Upper Implicit Schemes with Multiple Grids for the Euler Equations,* AIAA Journal, Vol. 25, 1987, pp. 929-935.

[6] Kroll, N. Radespiel, R. and Rossow, C.-C., *Experiences with Explicit Time-Stepping Schemes for Supersonic Flow Fields* Proceedings eighth GAMM Conference on Numerical Methods in Fluid Dynamics, Delft, 1989.

[7] Martinelli, L. and Jameson, A., *Validation of a Multigrid Method for the Reynolds Averaged Equations,* AIAA Paper 88-0414, 1988.

[8] Mulder, W.A., *A New Multigrid Approach to Convection Problems,* Journal Comput. Physics, Vol.83, pp.303-323, 1989.

[9] Pulliam, T. H., *Artificial Dissipation for the Euler Equations,* AIAA Journal, Vol.24, 1986, pp. 1931–1940.

[10] Radespiel, R. and Kroll, N., *A Multigrid Scheme with Semicoarsening for Accurate Computations of Viscous Flows* Proceedings Twelfth International Conference on Numerical Methods in Fluid Dynamics, Oxford, 1990.

[11] Shu, C.-W., *Total-Variation-Diminishing Time Discretizations* SIAM J. Sci. Stat. Comput., Vol. 9, 1988, pp.1073-1084.

[12] Swanson, R. C. and Turkel, E., *Artificial Dissipation and Central Difference Schemes for the Euler and Navier-Stokes Equations,* AIAA Paper 87-1107, AIAA 8th Computational Fluid Dynamics Conference, Honolulu, Hawaii, 1987.

[13] Swanson, R. C. and Turkel, E., *On Central Difference and Upwind Schemes,* ICASE Report 90-44, 1990, submitted to Journal of Comput. Physics

[14] Tadmor, E., *Convenient Total Variation Diminishing Conditions for Nonlinear Difference Schemes,* SIAM Journal of Numerical Analysis, Vol. 25, 1988, pp. 1002-1014.

[15] Tai, C.-H. *Optimizing the Coefficients for Multistage Central Difference Euler Schemes*, to be submitted to AIAA 10th CFD Conference, Honolulu, June 1991.

[16] Turkel, E., *Improving the Accuracy of Central Difference Schemes,* Springer-Verlag Lecture Notes in Physics, 11th International Conference on Numerical Methods in Fluid Dynamics, Vol. 323, 1988, pp. 586-591.

[17] Turkel, E. and Vatsa, V., *Effect of Artificial Viscosity on Three Dimensional Solutions,* AIAA paper 90-1444, 1990.

[18] Van Leer, B. Tai, C.-H. Powell, K.G. *Design of Optimally Smoothing Multi-stage Schemes for the Euler Equations* AIAA paper 89-1933-CP, 1989.

NASA
National Aeronautics and Space Administration

Report Documentation Page

1. Report No.	2. Government Accession No.	3. Recipient's Catalog No.
NASA CR-182082 ICASE Report No. 90-54		

4. Title and Subtitle	5. Report Date
MULTIGRID FOR HYPERSONIC INVISCID FLOWS	August 1990
	6. Performing Organization Code

7. Author(s)	8. Performing Organization Report No.
Naomi H. Decker Eli Turkel	90-54
	10. Work Unit No.
	505-90-21-01

9. Performing Organization Name and Address	11. Contract or Grant No.
Institute for Computer Applications in Science and Engineering Mail Stop 132C, NASA Langley Research Center Hampton, VA 23665-5225	NAS1-18605
	13. Type of Report and Period Covered
12. Sponsoring Agency Name and Address	Contractor Report
National Aeronautics and Space Administration Langley Research Center Hampton, VA 23665-5225	14. Sponsoring Agency Code

15. Supplementary Notes

Langley Technical Monitor:
Richard W. Barnwell

Proc. of 3rd International Conference on Hyperbolic Problems, 1990, to appear.

Final Report

16. Abstract

We consider the use of multigrid methods to solve the Euler equations for hypersonic flow. We consider the steady state equations with a Runge-Kutta smoother based on the time accurate equations together with local time stepping and residual smoothing. We examine the effect of the Runge-Kutta coefficients on the convergence rate considering both damping characteristics and convection properties. We also show the importance of boundary conditions on the convergence rate for hypersonic flow. Also of importance are the switch between the second and fourth difference viscosity. Solutions are given for flow around a bump in a channel and flow around a biconic section.

17. Key Words (Suggested by Author(s))	18. Distribution Statement
multigrid, hypersonics, Euler equations	64 - Numerical Analysis Unclassified - Unlimited

19. Security Classif. (of this report)	20. Security Classif. (of this page)	21. No. of pages	22. Price
Unclassified	Unclassified	18	A03